Journal of Chromatography A, 1241 (2012) 60–68

Contents lists available at SciVerse ScienceDirect

Journal of Chromatography A

journal homepage: www.elsevier.com/locate/chroma

Enantioseparation and chiral recognition mechanism of new chiral derivatives of xanthones on macrocyclic antibiotic stationary phases

Carla Fernandes[a,b], Maria Elizabeth Tiritan[a,c], Quezia Cass[d], Visvaldas Kairys[e], Miguel Xavier Fernandes[e], Madalena Pinto[a,b,*]

[a] Centro de Química Medicinal da Universidade do Porto (CEQUIMED-UP), Rua de Jorge Viterbo Ferreira 228, 4050-313 Porto, Portugal
[b] Laboratório de Química Orgânica e Farmacêutica, Departamento de Ciências Químicas, Faculdade de Farmácia, Universidade do Porto, Rua de Jorge Viterbo Ferreira 228, 4050-313 Porto, Portugal
[c] Centro de Investigação em Ciências da Saúde, Instituto Superior de Ciências da Saúde-Norte, (CICS-ISCS-N), Rua Central de Gandra 1317, 4585-116 Gandra PRD, Portugal
[d] Departamento de Química, Universidade Federal de São Carlos, SP, Rodovia Washington Luís (SP-310), km 235 – São Carlos, SP, Brasil
[e] Centro de Química da Madeira, Universidade da Madeira, Campus da Penteada, 9000-390 Funchal, Portugal

ARTICLE INFO

Article history:
Received 9 February 2012
Received in revised form 28 March 2012
Accepted 2 April 2012
Available online 11 April 2012

Keywords:
Macrocyclic antibiotic
Chiral stationary phases
Chiral derivatives of xanthones
Enantioselectivity
Enantiomeric purity
Chiral recognition

ABSTRACT

A chiral HPLC method using four macrocyclic antibiotic chiral stationary phases (CSPs) has been investigated for determination of the enantiomeric purity of fourteen new chiral derivatives of xanthones (CDXs). The separations were performed with the CSPs Chirobiotic T, Chirobiotic TAG, Chirobiotic V and Chirobiotic R under multimodal elution conditions (normal-phase, reversed-phase and polar ionic mode). The analyses were performed at room temperature in isocratic mode and UV and CD detection at a wavelength of 254 nm. The best enantioselectivity and resolution were achieved on Chirobiotic R and Chirobiotic T CSPs, under normal elution conditions, with R_S ranging from 1.25 to 2.50 and from 0.78 to 2.06, respectively. The optimized chromatographic conditions allowed the determination of the enantiomeric ratio of eight CDXs, always higher than 99%. In order to better understand the chromatographic behavior at a molecular level, and the structural features associated with the chiral recognition mechanism, computational studies by molecular docking were carried out using VDock. These studies shed light on the mechanisms involved in the enantioseparation for this important class of chiral compounds.

1. Introduction

The development of efficient methodologies to obtain both enantiomers with high enantiomeric purity is a very important task, especially in early stages of drug development. In this context, the use of HPLC with chiral stationary phases (CSPs) has proven to be the most helpful among the currently methods to achieve chiral separations and to measure the enantiomeric ratio [1,2]. On the other hand, macrocyclic antibiotic CSPs, introduced in 1994 by Armstrong et al. [3], became versatile and selective tools for the enantioresolution, evaluation of the enantiomeric purity and pharmacokinetic studies of different classes of chiral compounds [4–9]. The success of these CSPs can be associated with the diversity of their structures that contain a variety of functional groups, multiple stereogenic centers and inclusion cavities [10]. Furthermore, the possibility to perform at multimodal conditions, associated with their complementarily in selectivity profiles, increases their usefulness and applicability. So, nowadays the macrocyclic antibiotic CSPs are pointed out as one of the most versatile and robust CSPs [8].

In the past few years, several computational studies concerning chromatographic parameters have demonstrated to be very useful to understand the chiral recognition phenomenon of a variety of CSPs [11–18]. However, in spite of several studies regarding the structure of macrocyclic antibiotic CSPs [8,10,19–23], their physicochemical properties [8,10,20], applications [8,10,19,21], effect of the type of mobile phase [19,21,24] as well as thermodynamic investigations [25–27], relatively little is known in detail about their chiral recognition mechanisms at molecular level. It seems that the mechanism of chiral recognition is still not fully elucidated because of the structural complexity of the selectors which make investigations more complicated than with other selectors. Moreover, there are probably several kind of mechanisms that can contribute to the chiral recognition and subsequent retention, which depend not only on the nature of macrocyclic antibiotic CSP, but also of the structure of the analyte and on the elution chromatographic conditions [10]. Nonetheless, Bauvais et al. reported the elucidation of chiral recognition processes of nonsteroidal

* Corresponding author at: Centro de Química Medicinal da Universidade do Porto (CEQUIMED-UP), Rua de Jorge Viterbo Ferreira 228, 4050-313 Porto, Portugal. Tel.: +351 222078692; fax: +351 226093390.
E-mail addresses: madalena@ff.up.pt, madalenakijjoa@gmail.com (M. Pinto).

0021-9673/$ – see front matter © 2012 Elsevier B.V. All rights reserved.
http://dx.doi.org/10.1016/j.chroma.2012.04.011

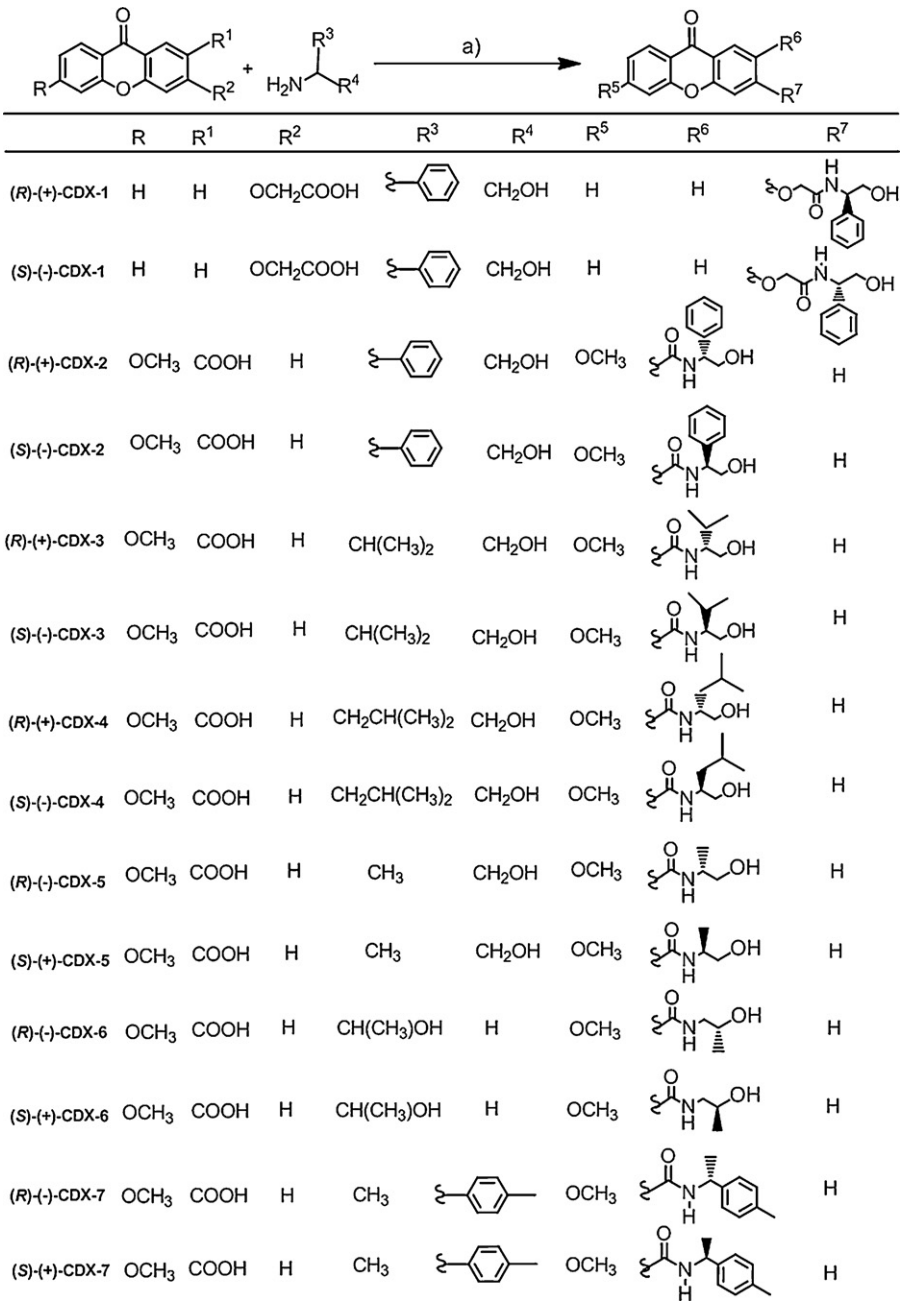

Fig. 1. Synthesis of (*R*)-(+) and (*S*)-(−)-CDX-1 (*N*-(2-hydroxy-1-phenylethyl)-2-((9-oxo-9*H*-xanthen-3-yl)oxy)acetamide); (*R*)-(+) and (*S*)-(−)-CDX-2 (*N*-(2-hydroxy-1-phenylethyl)-6-methoxy-9-oxo-9*H*-xanthene-2-carboxamide); (*R*)-(+) and (*S*)-(−)-CDX-3 (*N*-(1-hydroxy-3-methylbutan-2-yl)-6-methoxy-9-oxo-9*H*-xanthene-2-carboxamide); (*R*)-(+) and (*S*)-(−)-CDX-4 (*N*-(1-hydroxy-4-methylpentan-2-yl)-6-methoxy-9-oxo-9*H*-xanthene-2-carboxamide); (*R*)-(−) and (*S*)-(+)-CDX-5 (*N*-(1-hydroxypropan-2-yl)-6-methoxy-9-oxo-9*H*-xanthene-2-carboxamide); (*R*)-(−) and (*S*)-(+)-CDX-6 (*N*-(2-hydroxypropyl)-6-methoxy-9-oxo-9*H*-xanthene-2-carboxamide); (*R*)-(−) and (*S*)-(+)-CDX-7 (6-methoxy-9-oxo-*N*-(1-(*p*-tolyl)ethyl)-9*H*-xanthene-2-carboxamide). Reagents and conditions: (a) TBTU, triethylamine, dry tetrahydrofuran, room temperature, 30 min to 3 h.

anti-inflammatory drugs, anti-neoplastic compounds and *N*-derivatized amino acids on vancomycin selector by docking studies and molecular dynamics simulations [28].

Due to their biological properties, the importance of xanthone (9*H*-xanthon-9-one) derivatives is well recognized in Medicinal Chemistry [29]. Considering that our group has a vast experience in synthesis and biological evaluation of xanthone derivatives [30–36]; some chiral members of this family are promising compounds for diverse biological/pharmacological activities [29,37–40]; and that the examples of synthetic chiral derivatives of xanthones (CDXs) described are scarce [37–40]; a small library of both enantiomers of new CDXs have been synthesized (Fig. 1) [41], their chiral enantioresolution evaluated in four macrocyclic antibiotic CSPs and the enantiomeric ratio measured.

The separations of the enantiomeric mixtures of CDXs were performed with the CSPs Chirobiotic T, Chirobiotic TAG, Chirobiotic V and Chirobiotic R (Fig. 2) under multimodal elution conditions (normal-phase, reversed-phase and polar ionic mode). The chromatographic conditions affording the best resolutions were used for the determination of the enantiomeric ratio of the new CDXs synthesized.

Additionally, in order to better understand the chromatographic parameters at a molecular level, and the structural features associated with the chiral recognition mechanism, computational

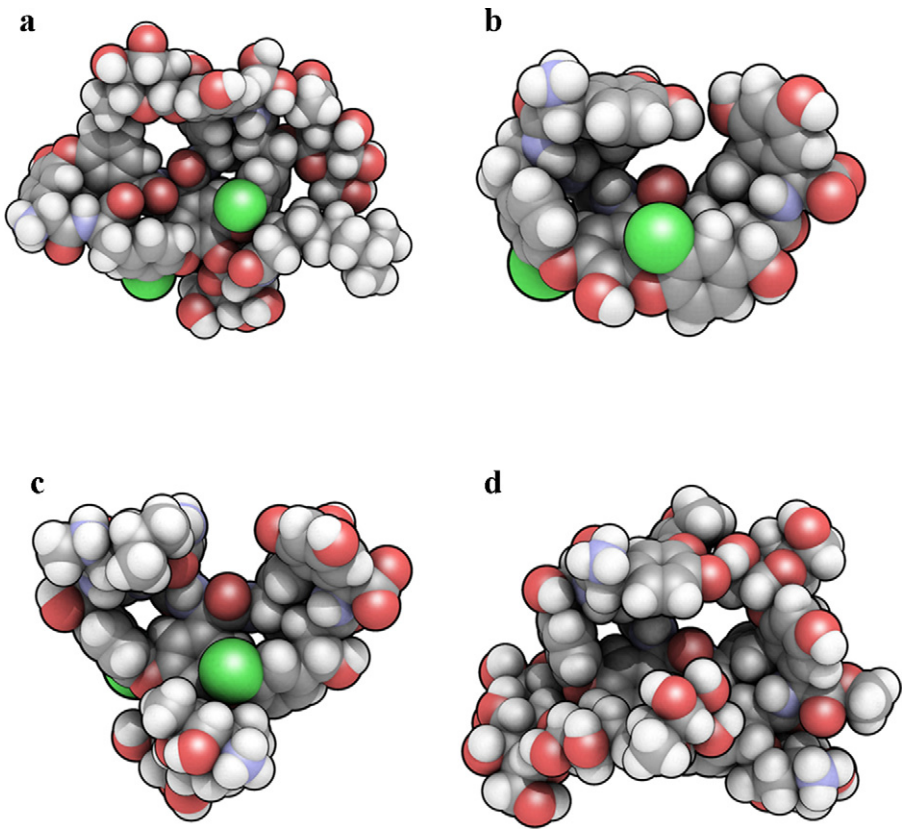

Fig. 2. The space-fill models of the macrocyclic antibiotic CSPs used in this study: (a) teicoplanin, (b) teicoplanin aglycon, (c) vancomycin, (d) ristocetin. The figure was produced using QuteMol [54].

modeling studies by molecular docking technique were carried out using VDock [42]. These studies shed light on the mechanisms involved in the enantioseparation and the results will be discussed in this work.

2. Experimental

2.1. Chemicals

CDXs were synthesized in our laboratory in enantiomeric pure form, by coupling carboxyxanthones with both enantiomers of commercially available chiral reagents (Fig. 1), according to the described procedure [41]. Methanol (MeOH), ethanol (EtOH), 2-propanol (2-prOH), *n*-hexane (Hex) for HPLC were purchased from Merck (Darmstadt, Germany). Triethylamine (TEA) and glacial acetic acid (AcOH) (both p.a. grade) were also obtained from Merck (Darmstadt, Germany). Ultrapure water was generated by a Milli-Q system (Millipore, Bedford, MA). The stock solutions of the CDXs were prepared by dissolution either in EtOH for separation at normal-phase elution conditions or in MeOH for polar ionic mode and reversed-phase mode at the concentration of 1 mg/mL and further diluted. Working solutions of enantiomeric mixture were prepared mixing equal aliquots of each enantiomer. The enantiomeric ratio determinations were performed with the stock solutions of each enantiomer of CDXs diluted at the concentration of 20 μg/mL. Solutions of 20 μg/mL of each enantiomer spiked with 1% of the opposite enantiomer were also prepared.

2.2. Instrumentation and operating conditions

The HPLC system used consisted of two Shimadzu LC 10-ADvp pumps, a FCV-10AL solvent selector valve, an automatic injector SIL10-Advp, a SPD-10AV UV/VIS detector with a SCL-10Avp interface. A CD detector model JASCO CD 2095 Plus was also used. Data acquisition was performed using Shimadzu LC SOLUTIONS software. A HPLC system consisted of one Shimadzu LC-10ATVP pump, equipped with a RHEODYNE 7725i injector fitted with a 100 μL loop, a SPD-10AV UV/VIS detector with a SCL-10Avp interface was also employed. Data acquisition was performed using Shimadzu CLASS-VP software.

The CSPs used in this study were Chirobiotic T (teicoplanin-bonded CSP), Chirobiotic TAG (teicoplanin aglycon-bonded CSP), Chirobiotic V (vancomycin-bonded CSP) and Chirobiotic R (ristocetin A-bonded CSP) (Fig. 2), all 15 cm × 4.6 mm i.d., particle size 5 μm except the Chirobiotic R (25 cm × 4.6 mm i.d., particle size 5 μm). These macrocyclic antibiotic CSPs were manufactured by ASTEC (Whippany, NJ, USA).

Analyses were performed at room temperature in isocratic mode. The flow rate used was 0.5 mL/min or 1 mL/min and the chromatograms were monitored by UV and CD detection at a wavelength of 254 nm. The sample injections (100 μL) were carried out in triplicate.

The solvents for mobile phases were filtered through a hydrophilic Durapore-GV membrane of 0.45 μm pore size from Millipore and were further degassed for 10 min in an ultrasonic bath before use. The mobile phase compositions were Hex and a modifier, EtOH or 2-prOH, for the normal-phase mode. In the polar ionic separation mode MeOH with several percentages of TEA and AcOH (0.01, 0.05, 0.1 or 1%) were used as mobile phases. Mixtures of different volume ratios of MeOH and 0.1 or 1.0% triethylamine acetate (TEAA) buffer, pH 4.0–6.2, were employed for the reversed-phase separation mode. TEAA buffers were prepared by titration of 0.1 or 1% (by volume) aqueous solutions of TEA with AcOH to adjust to a suitable pH.

Table 1
Chromatographic results obtained on Chirobiotic CSPs, under normal-phase elution conditions, for the enantiomeric mixtures of CDXs (1–5 and 7).

Enantiomeric mixture	Chirobiotic	Mobile phase (v/v)	k_1	α	R_S
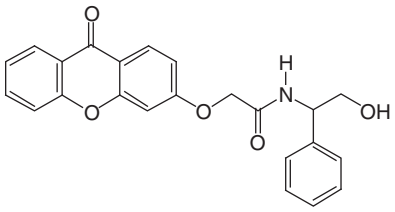 **CDX-1**	T	80/20	10.32	1.12	0.78
		70/30	5.12	1.12	0.73
		50/50	1.88	1.12	0.70
	TAG	60/40	14.40	1.07	0.60
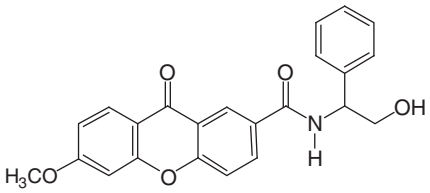 **CDX-2**	T	80/20	8.05	1.31	1.85
		70/30	4.01	1.35	1.29
		50/50	1.57	1.37	1.25
	R	40/60	0.77	1.49	2.34
		50/50	2.13	1.67	2.50
		50/50*	2.39	1.56	2.14
	V	80/20*	15.20	1.18	0.87
		70/30	6.33	1.19	0.94
		50/50	2.55	1.19	0.82
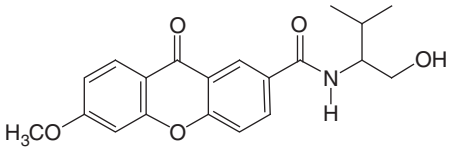 **CDX-3**	T	80/20	5.25	1.47	2.06
		70/30	2.43	1.46	1.83
		50/50	0.94	1.51	1.25
	R	40/60	0.55	1.31	1.25
		50/50	1.52	1.41	1.75
		50/50*	0.75	1.19	1.25
	V	80/20*	7.38	1.26	0.98
		70/30	3.08	1.27	1.12
		50/50	1.26	1.30	0.89
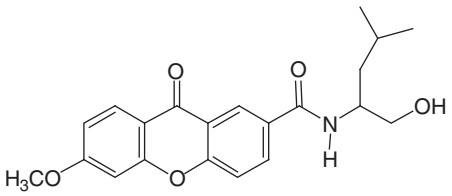 **CDX-4**	T	80/20	3.18	1.18	nc
		70/30	1.57	1.13	nc
	R	40/60	0.32	1.55	1.00
		50/50	0.97	1.36	1.53
		50/50*	0.44	1.62	1.00
	V	80/20*	4.47	1.19	0.60
		70/30	2.28	1.13	nc
		50/50	0.84	1.15	nc
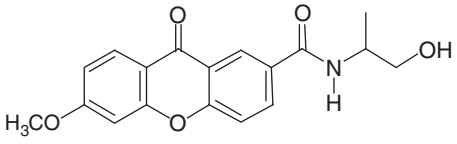 **CDX-5**	T	80/20	8.96	1.26	1.50
		50/50	1.44	1.29	1.00
	R	40/60	0.91	1.22	1.00
		50/50	2.32	1.27	1.25
	V	80/20*	11.05	1.15	0.83
		70/30	5.27	1.14	0.80
		50/50	2.03	1.13	nc
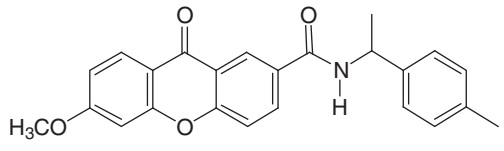 **CDX-7**	TAG	80/20*	13.09	1.09	nc

Chromatographic conditions: column, Chirobiotic T, TAG, R and V; mobile phase, Hex:EtOH (v/v); Flow rate, 0.5 mL/min or *1 mL/min; detection, 254 nm. nc: resolution was not calculated due to lack of accuracy caused by poor resolution.

Table 2
Best enantioresolution achieved on four macrocyclic antibiotic CSPs for enantiomeric mixtures of CDXs 1–5 and 7.

Enantiomeric mixture	Chirobiotic	Mobile phase	k_1	α	R_S
CDX-1	TAG	MeOH/AcOH/TEA: 100/0.5/0.5	0.79	1.18	0.80
CDX-2	R	Hex/EtOH: 50/50	2.13	1.67	2.50
CDX-3	T	Hex/EtOH: 80/20	5.25	1.47	2.06
CDX-4	R	Hex/EtOH: 50/50	0.97	1.36	1.53
CDX-5	T	Hex/EtOH: 80/20	8.96	1.26	1.50
CDX-7	V	MeOH/AcOH/TEA: 100/0.01/0.01	0.53	1.39	0.92

Hex: hexane; EtOH: ethanol; MeOH: methanol; TEA: triethylamine; AcOH: glacial acetic acid. Flow rate of 0.5 mL/min.

The column void time (t_0) was considered to be equal to the peak of the solvent front and was taken from each particular run. The enantiomeric ratio (er) was determined by the relative percentages of the peak areas according to [er (%) = $100 \times ([R] - [S]/([R] + [S])$ or $100 \times ([S] - [R]/([S] + [R])$, where [S] and [R] are the area of the peak of each enantiomer [43].

2.3. Computational

The 3D structures of the macrocyclic antibiotics were taken from the following Protein Data Bank (PDB) entries: 2XAD [44] (teicoplanin), 3MG9 [45] (teicoplanin aglycone), 1AA5 [46] (vancomycin). The Cambridge Crystallographic Data Centre (CCDC) entry 718620 [47] served as a source of the ristocetin A structure. CHARMm force field with Momany–Rone charges [48] for the macrocyclic antibiotic molecules were generated using Disovery Studio Visualizer v. 3.1 (Accelrys Software Inc., San Diego, CA) and were used during docking. The geometries of CDXs were generated using Vconf program (Verachem LLC, Gaithersburg, MD). During the docking, the modified Dreiding force field [49] and VeraChem's partial atomic charges [50] were used for the guest molecules.

Docking was performed with the Vdock program [42]. To better sample the surface of the host molecule, the default program settings were used, except for the number of docked minima (200 instead of 20), and the switching off of the Genetic Algorithm. The solvent effect was modeled with the distance-dependent dielectric approximation, $\varepsilon_{ij} = 4r_{ij}$ [51]. The host molecule was kept rigid during docking, while the dihedrals in the guest molecules were rotatable, except for the methyl groups.

3. Results and discussion

3.1. CSP and mobile phase selection

Under normal-phase elution conditions high enantioselectivity and resolution were achieved for four out of seven enantiomeric mixtures of CDXs, namely CDXs 2–5 (Table 1). Briefly, when Hex:EtOH (80:20 v/v) was used as mobile phase on Chirobiotic T good enantioselectivity ($\alpha = 1.31$) and resolution ($R_S = 1.85$) were obtained for enantiomeric mixture of CDX-2. However, with this mobile phase the retention factor was high ($k_1 = 8.05$). To overcome this situation, the polarity of the mobile phase was augmented (EtOH content increased from 20 to 50%) in order to consequently decrease the retention of the enantiomers, but resolution was decreased to $R_S = 1.25$. On the other hand, the Chirobiotic R CSP demonstrated excellent performance for enantioseparation of the enantiomeric mixture of CDX-2, mainly when Hex:EtOH (50:50 v/v) was used. In fact, it was the best enantioselectivity ($\alpha = 1.67$) and resolution ($R_S = 2.50$) achieved for this class of chiral compounds on all Chirobiotic CSPs evaluated. With the same mobile phase, the Chirobiotic R CSP also provided good enantioselectivity for enantiomeric mixture of CDX-3 ($\alpha = 1.41$) and CDX-5 ($\alpha = 1.27$). However, in spite of the good resolution obtained for enantiomeric mixture of CDX-3 ($R_S = 1.75$), for enantiomeric mixture of CDX-5 it was poor ($R_S = 1.25$). Furthermore, the Chirobiotic T was found to be the most successful CSP for the enantioseparation of these two enantiomeric mixtures (CDX-3 and CDX-5), using Hex:EtOH (80:20 v/v) as mobile phase, providing the highest enantioselectivity and resolution, with $\alpha = 1.47$, $R_S = 2.06$ and $\alpha = 1.26$, $R_S = 1.50$, respectively.

Concerning enantiomeric mixture of CDX-4, it could only be baseline resolved on the Chirobiotic R CSP, using the mobile phase composed of 50% EtOH, with good enantioselectivity ($\alpha = 1.36$) and resolution ($R_S = 1.53$).

Therefore, it was found that under normal-phase elution conditions, the Chirobiotic V CSP generally presented poor resolutions for all CDXs evaluated. Nevertheless, $\alpha = 1.27$ and $R_S = 1.12$ were achieved for enantiomeric mixture of CDX-3 using Hex:EtOH (70:30 v/v) as mobile phase. Moreover the Chirobiotic TAG CSP showed the worst performance for the separation of enantiomeric mixture of CDXs under these chromatographic conditions.

Generally, under the polar ionic mode of elution the chromatographic results were not satisfactory (data not shown); very low retention factors and absence or poor resolutions were obtained for all enantiomeric mixtures of CDXs on the four Chirobiotic CSPs evaluated. Thus, under these elution conditions, only some enantioselectivity was observed on Chirobiotic R, V and TAG CSPs for enantiomeric mixtures of CDX-2, CDX-7 and CDX-1 respectively, although with poor resolution. Nevertheless, for enantiomeric mixtures of CDX-1 and CDX-7 the enantioselectivity and resolution values achieved were the highest, with $\alpha = 1.18$, $R_S = 0.80$ and $\alpha = 1.39$, $R_S = 0.92$, respectively (Table 2). The very short retentions of the enantiomers of all CDXs in this elution mode might justify these chromatographic results.

Considering evaluation on the reversed-phase elution conditions the chromatographic results were also not satisfactory (data not shown). High retention time was observed, usually more than 60 min, with absence or very poor resolutions. The best resolution achieved in these conditions was $Rs = 0.70$ for the enantiomeric mixture of CDX-7 on Chirobiotic TAG using MeOH:1%TEAA pH = 6.0 (60:40 v/v) as mobile phase.

The optimized chromatographic conditions that allowed the best enantioresolutions for enantiomeric mixtures of CDXs (1–5 and 7) are summarized in Table 2. The enantiomeric mixture of CDX-6 was the only one for that all macrocyclic antibiotic CSPs used did not demonstrated enantioselectivity, obtaining only a single peak in all conditions evaluated.

As shown in Table 2, six of the seven enantiomeric mixtures of CDXs analyzed (1–5 and 7) were separated on antibiotic macrocyclic CSPs and four enantiomeric mixtures of CDXs (2–5) were baseline enantioseparated. Excellent resolutions were achieved for enantiomeric mixtures of CDXs 2 and 3 on Chirobiotic R and Chirobiotic T CSPs, respectively. These CSPs were also useful for the separation of the enantiomeric mixture of CDXs 4 and 5, providing good resolution. Enantiomeric mixtures of CDXs 1 and 7 were partially resolved under polar ionic mode on Chirobiotic TAG and Chirobiotic V CSPs, respectively. The results demonstrated that Chirobiotic R and Chirobiotic T CSPs under normal-phase conditions were the most efficient CSPs for chiral separation of this class of compounds.

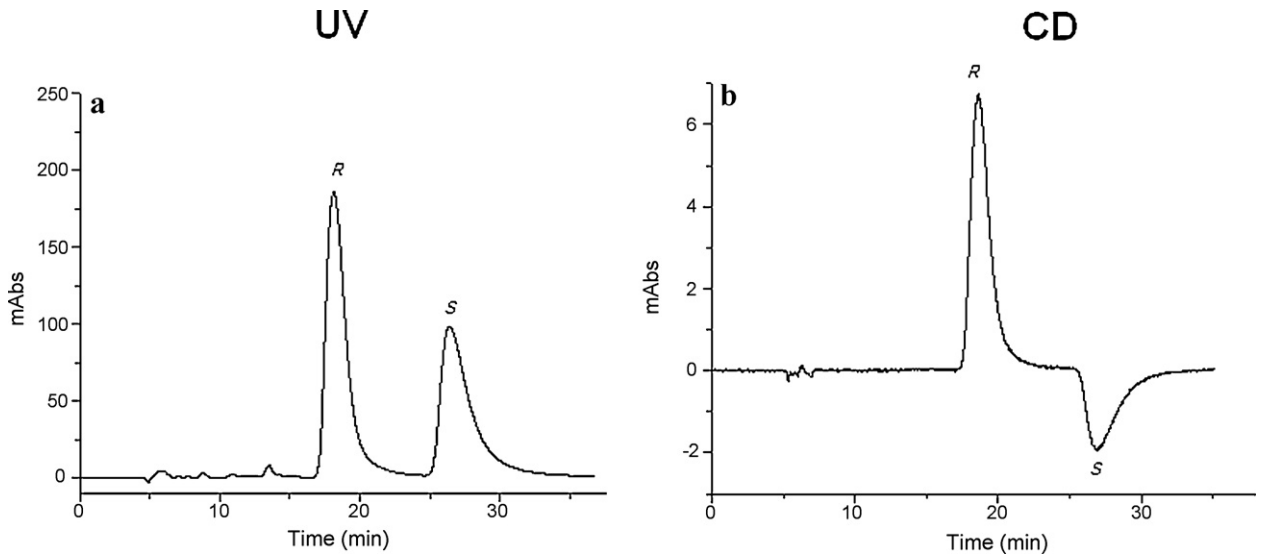

Fig. 3. UV (a) and CD (b) chromatograms of enantiomeric mixture of CDX-2. Chromatographic conditions: column, Chirobiotic R; mobile phase, Hex/EtOH: 50/50 (v/v); flow rate, 0.5 mL/min; detection, 254 nm.

In spite of the fact that polar organic, polar ionic and reversed-phase are, normally, the most successful elution modes with macrocyclic antibiotic CSPs [20], in this study the normal-phase demonstrated to be the most effective. It is well established that the molecular interactions depend critically on the stationary phase, on the mobile phase as well as on the nature of the analytes [19,20]. Considering that structures of the selectors include carboxylic acids and amines, for ionizable enantiomers these ionic functionalities perform strong interactions under reversed and polar ionic mode [20]. However, in this study all chiral compounds presented a xanthonic scaffold, amide and alcohol functional groups (except CDX-7, which has only an amide), which may explain the best resolutions under normal-phase conditions, suggesting that the π–π interactions and hydrogen bonding play important roles.

Characteristic chromatograms at optimized elution conditions for the enantiomeric mixture of CDX-2 are depicted in Fig. 3.

3.2. Determination of the enantiomeric ratio

After the systematic study of enantioresolution, the determination of the enantiomeric ratio (er) was performed using the chromatographic conditions associated with the best enantioresolution (Table 2). Fig. 4 shows characteristic chromatograms obtained during the method development for the measuring of the er of the CDXs enantiomers. CDX-3 was chosen to exemplify the determination of the er of each enantiomer. The optimized chiral HPLC conditions developed allowed the accurate determination of the er of each enantiomer of CDXs 2-5, always higher than 99%. The er was not determined for the enantiomers of CDXs 1 and 7, because the resolution achieved for these compounds was lower than 1.00.

The elution order was determined for the enantiomers of CDXs 2–5 by injecting the solutions of the enantiomeric mixtures, and then each enantiomer separately, under the optimized chromatographic conditions (Table 2). Under these elution conditions the (*R*)-enantiomer was the first to elute in all cases.

3.3. Docking studies

To further analyze the results, each enantiomer of CDX-1 to CDX-7 were docked into the investigated macrocyclic antibiotic CSPs using Vdock [42]. The docking calculation looked for the energy minima of the guest (ligand) and host (receptor) molecule complex where the energy function to be minimized is written as:

$$E_{\text{pot}} = E_{\text{vdW}} + E_{\text{el}} + E_{lig} \quad (1)$$

where E_{vdW} and E_{el} are the van der Waals and electrostatic interaction energies, respectively, between the guest and host, and E_{lig} is the intramolecular energy of the guest molecule. It has been shown

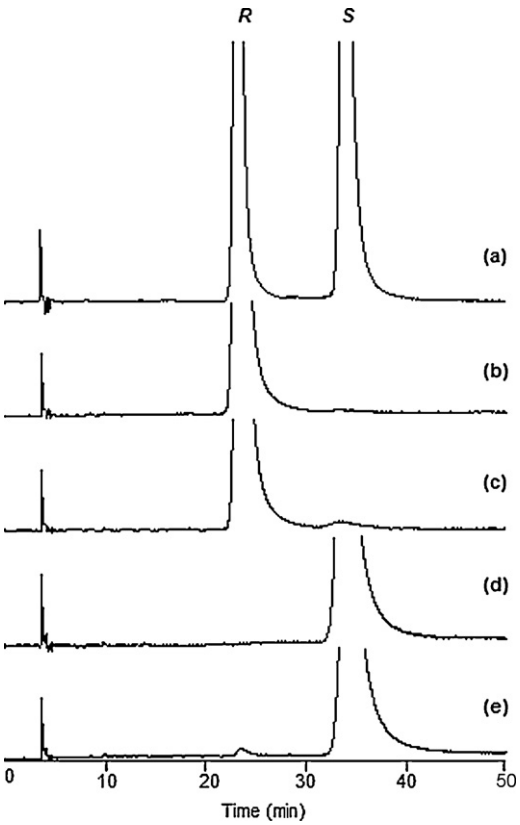

Fig. 4. (a) Chromatogram of enantiomeric mixture of CDX-3; (b) chromatogram of (*R*)-(+)-CDX-3; (c) chromatogram of (*R*)-(+)-CDX-3 spiked with 1% of (*S*)-(−)-CDX-3; (d) chromatogram of (*S*)-(−)-CDX-3; and (e) chromatogram of (*S*)-(−)-CDX-3 spiked with 1% of (*R*)-(+)-CDX-3. Chromatographic conditions: column, Chirobiotic T; mobile phase, Hex/EtOH: 80/20 (v/v); flow rate, 0.5 mL/min; detection, 254 nm.

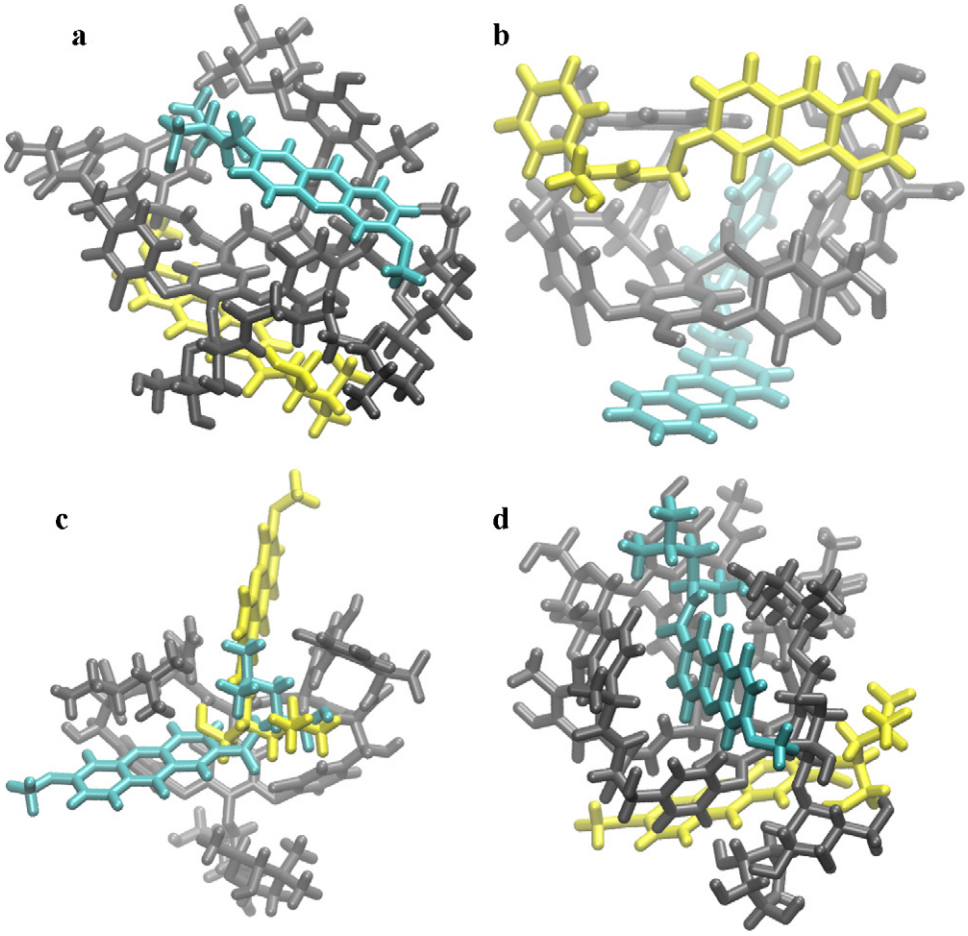

Fig. 5. Typical conformations of CDXs docked to the investigated CSPs: (a) teicoplanin and (*S*)-(−)-CDX-3, (b) teicoplanin aglycone and (*R*)-(+)-CDX-1, (c) vancomycin and (*R*)-(+)-CDX-4, (d) ristocetin and (*S*)-(−)-CDX-4 The host molecules are shown as dark gray sticks. The lowest energy conformations of CDXs are depicted as cyan sticks. Typical alternative conformations of docked CDXs are shown as yellow sticks, one per each guest-host pair to avoid clutter. The particular CDXs shown in the figure were chosen because they form the lowest energy during the docking compared with of the rest of guest molecules. (For interpretation of the references to color in this figure legend, the reader is referred to the web version of the article.)

previously, that theoretical calculations, and docking in particular, were able to predict the correct sign of the chiral separation, if a sufficiently number of conformations of the host/guest complex are sampled and the model is accurate enough [11]. In our calculations, we obtained 200 docked conformations (poses) for each CDX and CSP pair. The translational boxes were set sufficiently large to allow the guest molecule to choose the energetically preferred position over the entire surface of the host molecule, and the Genetic Algorithm was kept switched off during the calculation to make the potential energy surface sampling more random. To compute the estimate of the free energy of the complex, a predominant states approximation [52] was used:

$$A^{\circ} \approx -\mathrm{RT} \ln \left(\sum_{j=1}^{M} e^{-Ej/\mathrm{RT}} \right) \quad (2)$$

which includes contributions from the *M* number of lowest energy potential wells. Each of the macrocyclic antibiotics possesses a somewhat different shape of the surface cavity (Fig. 2): Chirobiotic V has a rather deep and short groove, Chirobiotic R – deep and narrow, Chirobiotic T – long and narrow, Chirobiotic TAG – short and shallow. These features had an effect on the distributions of the docked geometries of the guest molecules. Fig. 5 shows examples of the docked conformations for one of the guest molecules with all investigated macrocyclic antibiotic CSPs. For the larger Chirobiotics, T and R, the majority of low energy hits are concentrated in the binding groove of the molecule (cyan sticks in Fig. 5a, d). In the relatively small Chirobiotic V molecule, the guest molecules tend to bind inside of the rather deep binding groove (cyan sticks in Fig. 5c), but some guest molecules are also wedged in the "notch" of vancomycin molecule (yellow sticks in Fig. 5c). When docked to Chirobiotic TAG, because of the small size of the binding groove the guest molecules mostly position themselves around the outer surface (cyan sticks in Fig. 5b), stacking at the same time against the aromatic rings of Chirobiotic TAG.

The docked energies and the calculated free energies of the complex are reported in Table 3. The magnitudes of the computed energies, on average, are ranked as follows: Chirobiotics R < T < V < TAG. Complexes with Chirobiotic R have the lowest energies because of large size of the molecule and the deep binding groove. Chirobiotic V, though smaller in size, binds to CDXs better than Chirobiotic TAG. The low binding energies calculated for Chirobiotic TAG could probably be a result of the shallowness of its binding groove, which can also explain the poor experimental resolution obtained for this CSP. A shallow binding groove of the CSP also allows more interactions of the CDXs with the solvent and retention could be supplanted by these interactions with the solvent [53]. Chirobiotic R and Chirobiotic T molecules are significantly larger and thus can make more extensive van der Waals contacts compared to Chirobiotic V and Chirobiotic TAG.

Table 3
Docked energies E_{pot} and their components E_{vdW} and E_{el} (Eq. (1)), and the estimated free energies A° (Eq. (2)) for all CDXs and CSPs combinations.

	(*R*)-enantiomer				(*S*)-enantiomer				$A^{\circ}_R - A^{\circ}_S$	R_S
	E_{pot}	E_{vdW}	E_{el}	A°	E_{pot}	E_{vdW}	E_{el}	A°		
Chirobiotic T										
CDX-1	−30.73	−29.05	−5.08	−30.86	−29.27	−26.78	−4.32	−29.85	−1.01	0.78
CDX-2	−28.44	−25.49	−4.69	−29.27	−28.39	−26.35	−2.54	−29.49	0.22	1.85
CDX-3	−30.41	−25.17	−5.89	−31.05	−31.89	−24.49	−6.16	−32.02	0.97	2.06
CDX-4	−31.47	−24.70	−5.75	−31.71	−30.59	−27.49	−2.98	−31.15	−0.56	–
CDX-5	−27.93	−22.57	−4.98	−28.90	−29.55	−22.03	−6.81	−29.67	0.77	1.50
CDX-6	−29.54	−26.68	−3.38	−30.12	−28.71	−26.43	−4.38	−29.93	−0.19	–
CDX-7	−27.95	−26.30	−4.20	−28.98	−28.95	−27.74	−3.03	−29.62	0.64	–
Chirobiotic TAG										
CDX-1	−24.45	−23.97	−2.51	−24.46	−23.45	−21.20	−6.29	−23.67	−0.79	0.60
CDX-2	−23.34	−21.62	−3.26	−23.60	−22.79	−25.08	−0.98	−23.16	−0.44	–
CDX-3	−21.51	−17.37	−2.36	−21.85	−22.24	−15.99	−6.48	−22.67	0.82	–
CDX-4	−23.76	−21.43	−1.56	−24.05	−21.25	−18.82	−2.04	−22.07	−1.98	–
CDX-5	−19.80	−16.79	−1.86	−20.36	−20.63	−18.56	−1.92	−21.20	0.84	–
CDX-6	−21.08	−16.48	−3.47	−21.57	−20.80	−19.21	−1.32	−21.44	−0.13	–
CDX-7	−21.57	−21.17	−1.61	−21.98	−22.74	−23.44	−0.51	−22.91	0.93	–
Chirobiotic V										
CDX-1	−28.46	−25.88	−4.07	−29.41	−28.58	−25.78	−3.44	−29.48	0.07	–
CDX-2	−28.32	−25.44	−3.33	−28.94	−26.96	−24.28	−2.86	−28.01	−0.93	0.87
CDX-3	−28.62	−20.08	−7.12	−29.34	−28.00	−22.21	−6.06	−28.55	−0.79	0.98
CDX-4	−29.24	−26.76	−4.12	−30.16	−28.23	−24.24	−3.34	−28.97	−1.19	0.60
CDX-5	−27.29	−23.00	−3.64	−28.07	−26.85	−22.95	−3.40	−27.72	−0.35	0.83
CDX-6	−27.66	−20.77	−7.98	−28.40	−27.71	−24.11	−4.44	−28.58	0.18	–
CDX-7	−25.56	−23.82	−2.60	−26.88	−26.99	−25.18	−3.59	−27.72	0.84	–
Chirobiotic R										
CDX-1	−32.93	−32.53	−2.36	−33.95	−32.03	−33.49	−1.12	−33.03	−0.92	–
CDX-2	−32.73	−32.59	−3.41	−33.79	−33.10	−32.01	−3.33	−33.53	−0.26	2.34
CDX-3	−33.83	−31.85	−1.99	−34.50	−33.94	−29.26	−3.27	−35.23	0.73	1.75
CDX-4	−34.37	−30.48	−4.35	−35.11	−35.76	−32.32	−3.95	−36.55	1.44	1.53
CDX-5	−31.94	−27.90	−3.55	−32.89	−32.59	−28.28	−3.54	−34.07	1.18	1.25
CDX-6	−31.81	−29.90	−1.50	−32.95	−32.84	−30.35	−2.88	−33.86	0.91	–
CDX-7	−31.70	−32.70	−1.86	−32.48	−32.09	−33.13	−2.07	−32.97	0.49	–

The calculated free energy A° differences (Table 3) can be used to estimate the resolution for each CDX and CSP pair (negative energies will give resolutions below 1). As it can be seen from Table 3, calculations correctly predict the magnitude of the resolution for Chirobiotic T (4 cases), Chirobiotic TAG (1 case), Chirobiotic V (4 cases), and Chirobiotic R (3 cases). The calculations only fail to predict correctly the resolution of Chirobiotic R/CDX-2 complexes. Thus the prediction success rate is 92%, for the cases where an experimental value of resolution is available, which is rather satisfactory, having in mind the approximations that were used in this model, the most important among them being: rigid model for the receptor; simple distance dependent dielectric model, which is a rather crude approximation of the mobile phase; and neglect of entropy effects [11]. The docking results still provide values for the cases where experimental resolution was not achieved, which diminishes the predictability power of docking calculations. Overall, we can say that using this rather simple docking approach, it is possible to predict the correct enantiomer selection with a useful accuracy. Based on the observed results, it can be inferred that the general chemical structure and not solely the stereogenic center of the CDXs play an important role in the overall retention by the CSPs.

4. Conclusions

The separation of the enantiomers of new CDXs using macrocyclic antibiotic CSPs was evaluated on multimodal conditions. Six of the seven enantiomeric mixtures of CDXs (1–5 and 7) were separated. The best enantioselectivity and resolution were achieved on Chirobiotic R CSP for the enantiomerc mixture of CDX-2, using Hex:EtOH (50:50 v/v) as mobile phase, with $\alpha = 1.67$ and $Rs = 2.50$. A general rule could be established to describe the sequence of elution of the enantiomers of these compounds on macrocyclic antibiotic CSPs in normal elution condition. It was found that the (*R*)-enantiomer was the first to elute in all the cases (CDXs 2–5). The optimized chiral HPLC conditions were successfully employed for the accurate determination of the enantiomeric purity of eight CDXs, always higher than 99%. The docking calculations were able to estimate the resolution for CDXs with a success rate of 92%. The calculations also showed that each macrocyclic antibiotic CSP exhibits rather different binding patterns due to the shape and the surface of the chirobiotic CSP molecule.

Acknowledgements

This work was funded by FCT – Fundação para a Ciência e a Tecnologia under the project CEQUIMED-PEst-OE/SAU/UI4040/2011; under the project PEst-OE/QUI/UI0674/2011; under the project FCT-Grices/Capes 00770 29/05/08; and also funded by FEDER funds through the COMPETE program under the project FCOMP-01-0124-FEDER-011057.

References

[1] T.J. Ward, K.D. Ward, Anal. Chem. 82 (2010) 4712.
[2] A. Cavazzini, L. Pasti, A. Massi, N. Marchetti, F. Dondi, Anal. Chim. Acta 706 (2011) 205.
[3] D.W. Armstrong, Y. Tang, S. Chen, Y. Zhou, C. Bagwill, J.R. Chen, Anal. Chem. 66 (1994) 1473.
[4] M.M. Hefnawy, Y.A. Asiri, N.Z. Al-Zoman, G.A. Mostafa, H.Y. Aboul-Enein, Chirality 23 (2011) 333.
[5] L. Sipos, I. Ilisz, Z. Pataj, Z. Szakonyi, F. Fülöp, D.W. Armstrong, A. Péter, J. Chromatogr. A 1217 (2010) 6956.
[6] R. Berkecz, I. Ilisz, G. Benedek, F. Fülöp, D.W. Armstrong, A. Péter, J. Chromatogr. A 1216 (2009) 927.
[7] A.A. Al-Majed, J. Pharm. Biomed. Anal. 50 (2009) 96.
[8] T.J. Ward, A.B. Farris Iii, J. Chromatogr. A 906 (2001) 73.
[9] H.Y. Aboul-Enein, M.M. Hefnawy, H. Hoenen, J. Liq. Chromatogr. Related Technol. 27 (2004) 1681.

[10] I. Ilisz, R. Berkecz, A. Péter, J. Chromatogr. A 1216 (2009) 1845.
[11] K.B. Lipkowitz, J. Chromatogr. A 906 (2001) 417.
[12] M. Lämmerhofer, J. Chromatogr. A 1217 (2010) 814.
[13] A. Del Rio, J.M. Hayes, M. Stein, P. Piras, C. Roussel, Chirality 16 (2004) S1.
[14] A. Del Rio, P. Piras, C. Roussel, Chirality 17 (2005) S74.
[15] A. Del Rio, P. Piras, C. Roussel, Chirality 18 (2006) 498.
[16] C. Zhao, N.M. Cann, J. Chromatogr. A 1131 (2006) 110.
[17] C. Zhao, N.M. Cann, J. Chromatogr. A 1149 (2007) 197.
[18] C.F. Zhao, S. Diemert, N.M. Cann, J. Chromatogr. A 1216 (2009) 5968.
[19] T.E. Beesley, J.T. Lee, J. Liq. Chromatogr. Related Technol. 32 (2009) 1733.
[20] A. Berthod, Chirality 21 (2009) 167.
[21] A. Berthod, Y. Liu, C. Bagwill, D.W. Armstrong, J. Chromatogr. A 731 (1996) 123.
[22] A. Berthod, X. Chen, J.P. Kullman, D.W. Armstrong, F. Gasparrini, I. D'Acquarica, C. Villani, A. Carotti, Anal. Chem. 72 (2000) 1767.
[23] A. Péter, A. Árki, D. Tourwé, E. Forró, F. Fülöp, D.W. Armstrong, J. Chromatogr. A 1031 (2004) 159.
[24] K.H. Ekborg-Ott, Y. Liu, D.W. Armstrong, Chirality 10 (1998) 434.
[25] A. Berthod, B.L. He, T.E. Beesley, J. Chromatogr. A 1060 (2004) 205.
[26] A. Péter, G. Török, D.W. Armstrong, G. Tóth, D. Tourwé, J. Chromatogr. A 828 (1998) 177.
[27] T. Rojkovičová, J. Lehotay, D. Armstrong, J. Čižmárik, J. Liq, Chromatogr. Related Technol. 29 (2006) 2615.
[28] C. Bauvais, F. Barbault, Y. Zhu, M. Petitjean, B.T. Fan, SAR QSAR Environ. Res. 17 (2006) 253.
[29] M.M.M. Pinto, M.E. Sousa, M.S.J. Nascimento, Curr. Med. Chem. 12 (2005) 2517.
[30] A.M. Paiva, M.E. Sousa, A. Camões, M.S.J. Nascimento, M.M.M. Pinto, Med. Chem. Res. (2011) 1.
[31] A. Palmeira, M.H. Vasconcelos, A. Paiva, M.X. Fernandes, M. Pinto, E. Sousa, Biochem. Pharmacol. 83 (2012) 57.
[32] R.A.P. Castanheiro, M.M.M. Pinto, S.M.M. Cravo, D.C.G.A. Pinto, A.M.S. Silva, A. Kijjoa, Tetrahedron 65 (2009) 3848.
[33] R.A.P. Castanheiro, M.M.M. Pinto, A.M.S. Silva, S.M.M. Cravo, L. Gales, A.M. Damas, N. Nazareth, M.S.J. Nascimento, G. Eaton, Bioorg. Med. Chem. 15 (2007) 6080.
[34] C. Portela, C.M.M. Afonso, M.M.M. Pinto, D. Lopes, F. Nogueira, do RosárioF V., Chem. Biodivers. 4 (2007) 1508.
[35] E. Costa, E. Sousa, N. Nazareth, M.S.J. Nascimento, M.M.M. Pinto, Lett. Drug Des. Discovery 7 (2010) 487.
[36] M. Correia-Da-Silva, E. Sousa, B. Duarte, F. Marques, F. Carvalho, L.M. Cunha-Ribeiro, M.M.M. Pinto, J. Med. Chem. 54 (2011) 5373.
[37] E.P. Sousa, A.M.S. Silva, M.M.M. Pinto, M.M. Pedro, F.A.M. Cerqueira, M.S.J. Nascimento, Helv. Chim. Acta 85 (2002) 2862.
[38] H. Marona, N. Szkaradek, A. Rapacz, B. Filipek, M. Dybała, A. Siwek, M. Cegła, E. Szneler, Bioorg. Med. Chem. 17 (2009) 1345.
[39] M. Jastrzębska-Więsek, R. Czarnecki, H. Marona, Acta Pol. Pharm. Drug Res. 65 (2008) 591.
[40] H. Marona, N. Szkaradek, E. Karczewska, D. Trojanowska, A. Budak, P. Bober, W. Przepiórka, M. Cegla, E. Szneler, Arch. Pharm. (Weinheim) 342 (2009) 9.
[41] M. Pinto, M.E. Tiritan, C. Fernandes, Q. Cass, in Boletim da Propriedade Industrial no. 2011/01/21, Portugal, 2011.
[42] V. Kairys, M.K. Gilson, J. Comput. Chem. 23 (2002) 1656.
[43] R.E. Gawley, J. Org. Chem. 71 (2006) 2411.
[44] H.C. Chan, Y.T. Huang, S.Y. Lyu, C.J. Huang, Y.S. Li, Y.C. Liu, C.C. Chou, M.D. Tsai, T.L. Li, Mol. BioSyst. 7 (2011) 1224.
[45] M.J. Bick, J.J. Banik, S.A. Darst, S.F. Brady, Biochemistry (Mosc) 49 (2010) 4159.
[46] P.J. Loll, A.E. Bevivino, B.D. Korty, P.H. Axelsen, J. Am. Chem. Soc. 119 (1997) 1516.
[47] V. Nahoum, S. Spector, P.J. Loll, Acta Crystallogr. D 65 (2009) 832.
[48] F.A. Momany, R. Rone, J. Comput. Chem. 13 (1992) 888.
[49] S.L. Mayo, B.D. Olafson, W.A. Goddard Iii, J. Phys. Chem. 94 (1990) 8897.
[50] M.K. Gilson, H.S.R. Gilson, M.J. Potter, J. Chem. Inf. Comput. Sci. 43 (2003) 1982.
[51] B.R. Gelin, M. Karplus, Biochemistry (Mosc) 18 (1979) 1256.
[52] M.K. Gilson, Proteins 15 (1993) 266.
[53] R.E. Boehm, D.E. Martire, D.W. Armstrong, Anal. Chem. 60 (1988) 522.
[54] M. Tarini, P. Cignoni, C. Montani, IEEE Trans. Vis. Comput. Gr. 12 (2006) 1237.